Inertial Navigation Electro-Optical Aiding During GPS Dropouts

Alison Brown and Dan Sullivan, *NAVSYS Corporation*

BIOGRAPHY

Alison Brown is the President and CEO of NAVSYS Corporation. She has a PhD in Mechanics, Aerospace, and Nuclear Engineering from UCLA, an MS in Aeronautics and Astronautics from MIT, and an MA in Engineering from Cambridge University. In 1986, she founded NAVSYS Corporation. Currently she is a member of the GPS-III Independent Review Team, the IGEB Independent Advisory Team, the Air Force Science Advisory Board and serves on the GPS World editorial advisory board.

Dan Sullivan is a Sr. Scientist at NAVSYS Corporation. He is responsible for GPS/INS integration algorithms, architecture and software. Previously he was employed as a Senior Staff Engineer with Lockheed Martin Missiles and Fire Control in Orlando, FL, where he was responsible for systems analysis and design for image-processing, target state estimation and sensor fusion for a variety of missile, fixed-wing and rotary-wing targeting systems. He has a MS in Electrical Engineering from Columbia University.

ABSTRACT

Inertial navigation with low-cost IMU's can be an acceptable sole navigation source during short periods of GPS signal dropout due to intentional or unintentional interference. However, as the dropout period continues, the inertial navigation error reach unacceptable levels. In this paper, a technique is presented where relative or absolute position estimates derived from onboard captured image data are used to update the inertial navigation solution during GPS dropouts. This optical aiding technique is described and test results shown from aircraft and ground-based navigation trials.

INTRODUCTION

Several military and commercial platforms are currently installing navigation sensors concurrently with the introduction of high quality visual capabilities and digital mapping/imagery databases. The Navigation/Electro-Optic Sensor Integration Technology (NEOSIT) software application, developed for CECOM, is designed to optimally integrate navigation data, sensor imagery and image or terrain database to estimate and correct for errors in each data source. The modular design is to allow the NEOSIT application to be used with sensors and navigation already installed on different host platforms and with digital mapping and imagery data sources with varying degrees of precision.

The NEOSIT software application is designed to operate in three modes. The first mode uses the precision GPS/inertial imagery metadata to extract target coordinates from the imagery. The second mode is used to correct for offsets in the image or terrain database registration coordinates. The third mode of operation is to provide a back-up navigation capability in the event of GPS drop-outs by applying reference points from the imagery to update the on-board navigation solution.
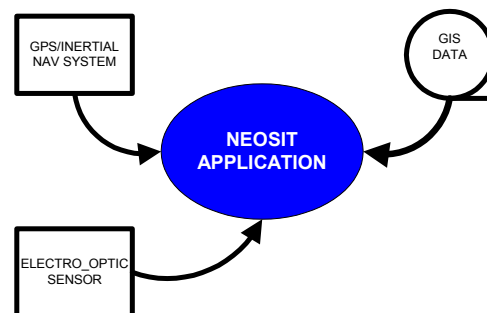
NEOSIT SOFTWARE APPLICATION

Figure 1 NEOSIT Component Interfaces

The NEOSIT application is designed to interface with the following components, as illustrated in Figure 1.

GPS/Inertial Navigation System

The integrated GPS/inertial navigation data is used to provide the geospatial reference data associated with the electro-optic sensor data. The results presented in this paper were generated using NAVSYS' GI-Eye product, shown in Figure 2. Examples of image rectification and target geo-location performance using the GI-Eye geospatial reference data are provided in reference [1].

Electro-Optic Sensor

The NEOSIT application can be used to process data from a variety of different sensors including optical, IR, or

hyperspectral devices. These sensors must only be capable of providing digital data in a standard image format to the NEOSIT application. The Hasselblad digital frame camera shown in Figure 2 was used to provide the test data presented in this paper.

GIS Geospatial Data
The NEOSIT application can accept data from a variety of different digital data sources including government and commercial. This includes rectified imagery, such as the Controlled Image Base® (CIB®), Digital Precision Point Data Base (DPPDD), digital terrain elevation data (DTED®) and vector maps (such as VMAP or commercial equivalents).
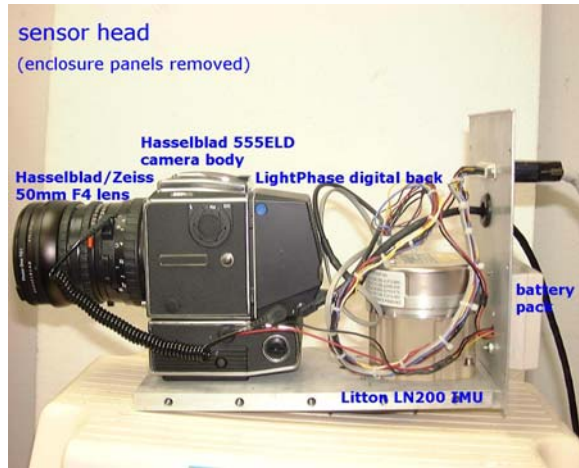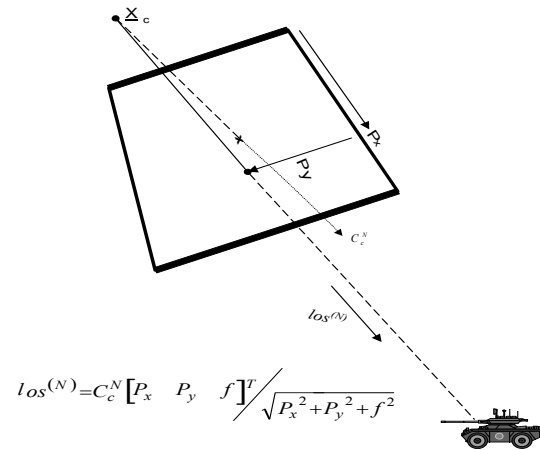

Figure 2 GI-Eye Product

$$los^{(N)} = C_c^N \begin{bmatrix} P_x & P_y & f \end{bmatrix}^T / \sqrt{P_x^2 + P_y^2 + f^2}$$

Figure 3 Measurement Geometry

GEOREGISTRATION ALGORITHM
The core algorithm for all of the modes of operation of the NEOSIT software is the georegistration algorithm shown in Figure 3. The estimated line-of-sight to any feature in the video image, derived in the navigation (North, East, Down) frame, can be computed by transforming the pixel derived line-of-sight vector in

camera axes to the navigation frame using the inertial attitude data.

$$\underline{l}^{(C)} = [p_x \quad p_y \quad f] / \sqrt{p_x^2 + p_y^2 + f^2} \quad \textbf{(1)}$$

$$\underline{l}^{(N)} = C_B^N C_C^B \underline{l}^{(C)} \quad \textbf{(2)}$$

Since the camera location is known ($\underline{x}_C$), the target coordinates can be calculated through a least squares solution from multiple image data. The observed line-of-sight to the target provides a measure of the offset between the estimated target location and the observed target location through the following equation.

$$\underline{x}_T^{(N)} = \underline{x}_C^{(N)} + R\,\underline{l}^{(N)} \qquad R = \left| \underline{x}_T - \underline{x}_C \right| \quad \textbf{(3)}$$

$$\underline{z} = \hat{\underline{x}}_T - \underline{x}_T = \hat{\underline{x}}_T - \underline{x}_C^{(N)} - R\,\underline{l}^{(N)}$$

This residual provides a measure of the following error sources:

- Error in the feature coordinates ($\hat{\underline{x}}_T$) (errors in the GIS data source)
- Error in the camera location ($\hat{\underline{x}}_C$) (errors in the navigation position solution)
- Error in the estimate of the camera attitude (C_B^N) (errors in the inertial attitude solution)

This observability is the key to the video estimation process, enabling both target location errors and navigation errors to be estimated from the integrated navigation and image data.

TARGET GEOLOCATION DATA
To evaluate the image georegistration accuracy of the NEOSIT system, imagery and navigation data was collected from an aircraft at a nominal altitude of 1000m AGL [1]. The camera field-of-view was 28 degrees, and the image resolution was 2032x3056, yielding a ground pixel resolution of about 23 cm/pixel. The collected imagery and associated navigation data were rectified and geo-registered using the ERDAS OrthoBase package in the Imagine™ software. The navigation data was used "as is", and no image tie-point processing was performed to improve the registration and rectification process. A portion of a rectified mosaic (with UTM coordinates) and a sample region containing three image-boundaries from the mosaic is shown Figure 4. (Although the quality of the image reproduction in this document is limited, it is hoped the reader can see that the mis-registration is on the order of a pixel). This result shows the capability of the GPS/inertial metadata to ortho-rectify airborne imagery with **no image tie-points** and **no image manipulation** in producing the rectified results.
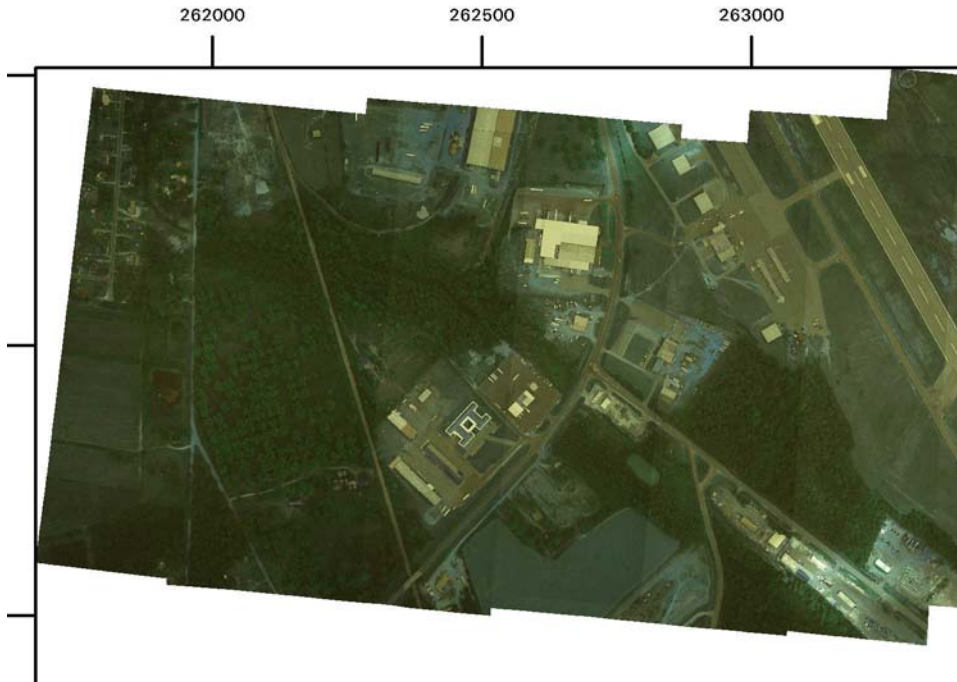
Figure 4 Rectified Mosaic Examples

Using the same flight data as referenced in the previous section, a series of surveyed targets had their geo-coordinates computed. These coordinates were derived by simply reading the latitude and longitude values in the rectified image mosaics. Table 1 summarizes the target geo-location performance of the system. In this configuration, the system was using a WAAS DGPS receiver system to provide RTCM pseudo-range correction data for input into InterNav. The targets were accurately surveyed with carrier-phase GPS, so the resulting targeting error is principally a combination of ownship position error and attitude error. Since the absolute position accuracy of DGPS is on the order of 1-1.5 meters, the 0.92 meter CEP from 1000m+ range indicates that, not only is the position solution good, but the attitude error is extremely small, clearly well under one mrad.

Table 1 Geo-Location Performance from Rectified Imagery

Point	Avg East Error (m)	Avg North Error (m)	Avg dist (m)
NSPL01	-0.11	-0.35	0.37
CPES Blueberry	0.43	-0.87	0.97
CPES Hort Hill	-0.49	-0.32	0.58
Tifton A – CoC	-0.35	-2.23	2.26
FAA TMA	0.20	1.14	1.16
Tifton CBL 150	-0.31	0.20	0.37
Tifton CBL 0	-0.15	0.28	0.32
Tifton CBL 100	-0.24	0.20	0.31
Excelsior reset	0.48	-1.77	1.83
M 157	0.65	1.80	1.91
Total RMS	0.47	1.27	0.92

VIDEO-AIDING NAVIGATION UPDATES
Coupling video and navigation data can serve several different purposes. When a good navigation solution is available, it can be used to build new waypoint models for later use or to improve the accuracy of existing GIS-based waypoint models. It can also be used to provide target geo-coordinates for any object of interest. When GPS is denied, the system can operate in two modes. First, it can use previously-stored waypoint models to provide absolute navigation updates, eliminating INS drift. Alternatively, it can create new waypoints even under GPS-denied conditions, which provide relative position-aiding to reduce INS drift.

The required pixel measurements for the video aiding process can come from manually-cued objects in the scene or from a waypoint detection algorithm which automatically detects and localizes waypoint objects. The following sections describe an automated approach to waypoint modeling and detection and describe the method used to apply these measurements for navigation updating.

Estimates are obtained by automatically localizing a model of a scene object, or landmark, in the image data. Accurate scene coordinates for the landmarks are required to generate absolute position estimates. These may be obtained from map data, or from the platform at times when accurate image sensor position and attitude estimates are available. For relative position estimates, the landmark is selected in one image, automatically modeled, and localized in subsequent images.

MODEL GENERATION AND LOCALIZATION
For position aiding, the operation of the system depends on the availability of a database of three-dimensional object models. These models can be generated using GIS data (vector maps or CIB/orthoquad imagery in conjunction with DTED) or imagery collected from a platform with accurate navigation equipment (e.g., when GPS is not denied). Figure 5 shows a block diagram of the Model Generation process.
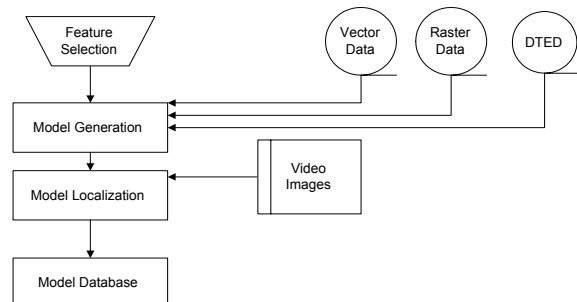

Figure 5 Model Generation and Localization Process

Model generation begins with the selection of a feature. From the GPS/inertial reference data, it is possible to estimate the viewing parameters of the imaging sensor. These meta-data can be used to compute the geographic region that is in the field view of the sensor. A query is then performed on the GIS data to aid in the determination of the range to the selected feature.

As shown in Figure 6, this approach results in a model that may have a large position uncertainty along the line-of-sight, depending on the accuracy of the information used to estimate the range to the feature. This error can be reduced by combining data from multiple images as discussed below.
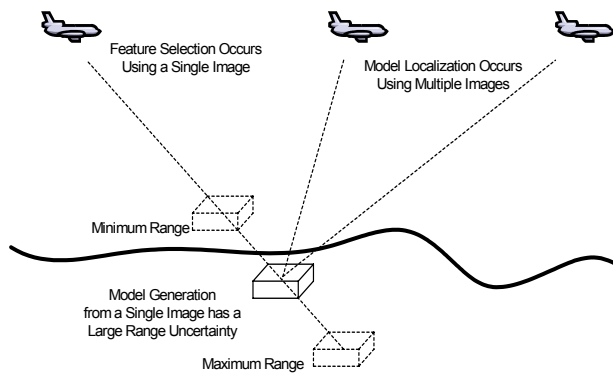
Figure 6 Model Generation and Localization

When an accurate navigation solution is available, the offset between the predicted feature location based on the GPS/inertial data and the actual location observed from within the video frame is a function of the error in the recorded location for that feature within the model database. If the specific model contained in the database was constructed using a single image and digital elevation map, the model position error will be principally along the line-of-sight in the original image. This line-of-sight is projected into subsequent images based on the platform navigation solution. It is then possible to search along the line-of-sight to locate the model in subsequent images. Multiple range hypotheses are calculated for the purposes of matching the model to multiple images. The results are used to improve the model contained in the database.

For GIS-base models, the location and attitude of each sensor image is used to compute a projection of the image onto the map and identify a region of interest within the database. A query is performed on the GIS data to identify any features that fall within this region. The features that are returned from this query are then processed by a feature extraction algorithm where their precise coordinates are detected within the image data.

To generate a model, a series of image-processing operations are performed which extract edges from the region of interest and look for salient line features using a Hough-transform-based algorithm[2,3]. Figure 7 shows an example of the model extracted from a building. The model is stored on-board as a simple list of line segment (lat/lon/alt) coordinates, greatly reducing storage requirements compared with image-based correlation approaches.
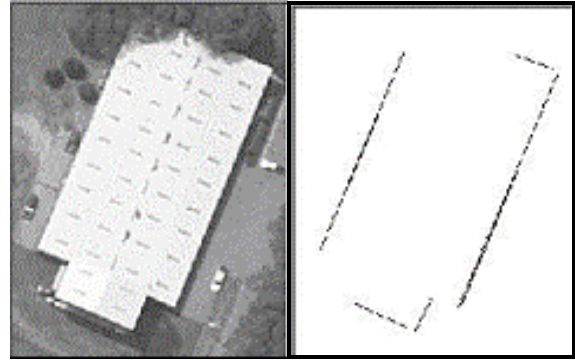

Figure 7 Model Extraction

Models can also be extracted directly from GIS vector products, bypassing the need for airborne reference data.

MODEL DETECTION

Given a pre-loaded or dynamically-extracted model, the navigation aiding process must then be able to localize that model within a scene. This match process uses a multiple-hypothesis chamfer-matching approach. Based on the current navigation (position and attitude) and model uncertainty, a region of interest (ROI) is selected which should contain the waypoint object. A distance transformation image is produced for each match image by first performing Canny edge detection on the region of interest and then computing a distance transformation. The distance transformation image or "distance map" is the input to the chamfer match function.[4,5] Edges appear as black pixels and other pixels appear lighter the farther they are from edges. A gradient descent function[6] is used to find the best match location between the model and the scene. To avoid spurious local minimum detections, multiple starting points are used in the distance map. Also, multiple models representing different range hypotheses can be applied to the same distance map at very little extra computational cost, allowing a large target uncertainty to be searched efficiently.
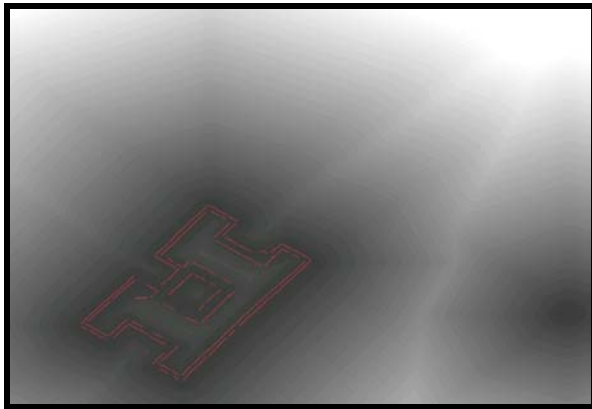
Figure 8 ROI and Detected Model

Figure 9 Gradient Descent in ROI Distance Map

Figure 8 and Figure 9 show an example of the results obtained from running the chamfer match function with an initial navigation error. The blue model denotes the expected model location at the center of a yellow uncertainty box derived from the model and navigation uncertainty. The red outline shows the minimum-error match location. The expected range-to-target is determined from DTED and the onboard navigation solution, with a corresponding level of uncertainty from both contributors. A series of range hypotheses are selected spanning this uncertainty. Corresponding hypotheses are generated, then projected into candidate images. The best target location match is then determined using the most likely hypothesis over a series of images.

A similar example using a model generated from a vector road database is shown in Figure 10. The complex surface of the distance image shows the utility of using multiple hypotheses for the starting point of the gradient-descent minimization.
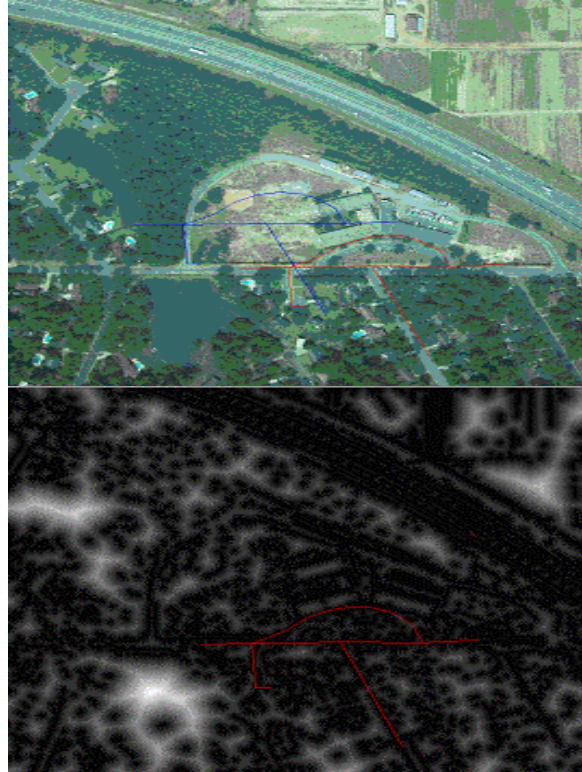

Figure 10 Detection of model derived from VMAP (top) expected and detected model in image (bot) model on distance map

NAVIGATION ERROR ESTIMATION
The pixel observation residual between the expected and measured model position can be used to observe both the target coordinate error and the navigation error. Observability of the navigation error requires multiple observations, either from multiple waypoints or to the same waypoint at different times during aircraft maneuver. To enable updates to be applied correctly from pixel observations taken at different times, the update equation takes into account the error propagation of the inertial error states between times, using standard state-transition matrix techniques. The internal navigation states that can be observed using this equation include the navigation solution errors and instrument errors. A minimum implementation would include three position states, three velocity states and three alignment error (ψ) states, or a total of N=9 states. Additional states are also included in the inertial Kalman Filter for accelerometer and gyroscope bias, scale factor and misalignment errors.

6

AIRBORNE TEST RESULTS

The aerial data shown earlier [1], was also used to test the Model Detection and Navigation Update algorithms. Models were generated of suitable landmarks in this area and the model update function was then used to localize the models using multiple images using the NEOSIT Target Geolocation capability. A second set of navigation data were then generated, without the use of GPS aiding, to emulate the effect of navigating through the same are in the event of GPS jamming.

Using the model detection algorithms described above, a navigation solution was computed using only INS data with image aiding. The NED-frame difference between the DGPS navigation solution and the image-aided navigation solution is shown in Figure 11.
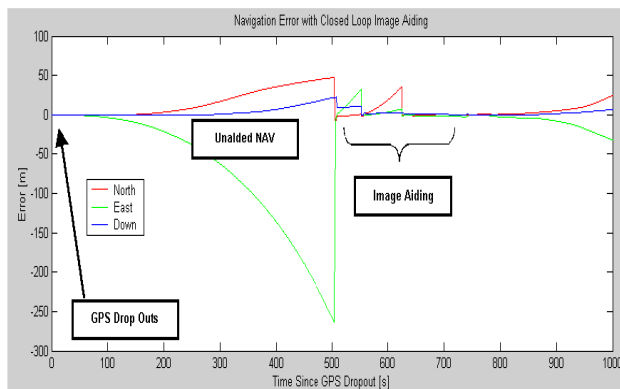

Figure 11 Airborne Navigation Performance with Image Aiding

For the first 500 seconds, no object models were in view, and the free-inertial navigation solution drifted away from truth. Once a model was visible, the estimation software applied a correction to the navigation solution. Note that, after this correction was applied, the error again began to accumulate but that the growth of the error with respect to time was reduced, indicating that position, velocity and attitude error were observed and reduced. As more models came into view, the error was better observed. At t=650 seconds, the error even approached the accuracy of the original DGPS-aided navigation solution despite having no GPS data for over ten minutes and image aiding in only the previous three minutes. In this test, no models were available after t=750 seconds, so the inertial solution again began to degrade after that time.

GROUND-BASED TEST RESULTS

A similar test was conducted with ground-based data. Figure 12 shows examples of the region-of-interest and measured detection image model, in this case a signpost.

Figure 12 Ground-based image aiding test

This single model was used for navigation updates during a period spanning the collection of twelve images. The result of this test is shown in Figure 13. Note that image updates were able to maintain the navigation error to less than one meter while the object model was in view. At t=100 seconds, the model was no longer in view and the navigation error began to accumulate.
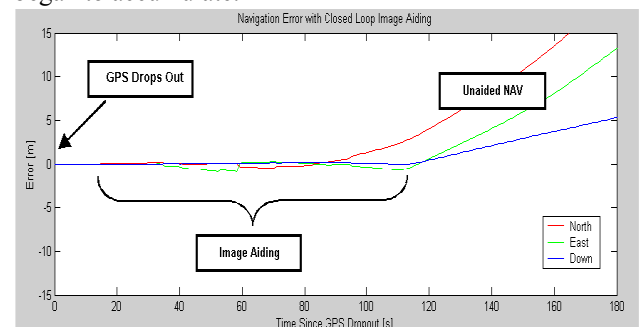

Figure 13 Ground Based Navigation Performance with Image Aiding

SUMMARY

The NEOSIT software application includes a combination of GPS/inertial navigation, image-processing and georegistration and navigation update functions that provides the ability to couple image measurements into the navigation solution to bound the inertial navigation solution drift when GPS dropouts occur, for example from jamming. The results using both terrestrial and aerial systems clearly demonstrate the ability of the system to observe the error present in the navigation solution using imagery and correct the navigation solution for the observed error. With as few as two or three video navigation updates per minute, an accurate navigation solution can be maintained using images that were previously registered with the GPS/inertial targeting system. When using CIB imagery or VMAP registered Models to apply the navigation updates, the accuracy of the final solution will also be affected by the registration quality of the reference data.

REFERENCES

[1] Sullivan, D. and Brown, A. "High Accuracy Autonomous Image Georeferencing Using a GPS/Inertial-Aided Digital Imaging System." Proceedings of the ION 2002 NTM, San Diego, CA.

[2] Canny, J. "A Computational Approach to Edge Detection," IEEE Transactions on Pattern Analysis and Machine Intelligence, Vol. 8, No. 6, November 1986, pp. 679-698.

[3] Hough, P.V.C. [1962]. "Methods and Means for Recognizing Complex Patterns." U.S. Patent 3,069,654.

[4] Barrow, H.G., Tenenbaum, J.M., Bolles, R.C., and Wolf, H.C. "Parametric Correspondence and Chamfer Matching: Two New Techniques for Image Matching." Proceedings of the 5th International Joint Conference on Artificial Intelligence, Cambridge, Massachusetts, 1977, pp 659-663.

[5] Borgefors, G. "Hierarchical Chamfer Matching: A Parametric Edge Matching Algorithm." IEEE Transactions on Pattern Analysis and Machine Intelligence, Vol. 10, No. 6, November 1988, pp. 849-865.

[6] MacLean, W.J., and Tsotsos, J.K.T. "Fast Pattern Recognition Using Gradient-Descent Search in an Image Pyramid." Proceedings of the 15th International Conference on Pattern Recognition, Barcelona, Spain, Sept. 2000.